AIP | Journal of Applied Physics

Dominant thermal boundary resistance in multi-walled carbon nanotube bundles fabricated at low temperature

Sten Vollebregt, Sourish Banerjee, Ann N. Chiaramonti, Frans D. Tichelaar, Kees Beenakker, and Ryoichi Ishihara

Citation: Journal of Applied Physics **116**, 023514 (2014); doi: 10.1063/1.4889820
View online: http://dx.doi.org/10.1063/1.4889820
View Table of Contents: http://scitation.aip.org/content/aip/journal/jap/116/2?ver=pdfcov
Published by the AIP Publishing

JOURNAL OF APPLIED PHYSICS 116, 023514 (2014)

Dominant thermal boundary resistance in multi-walled carbon nanotube bundles fabricated at low temperature

Sten Vollebregt,[1,a)] Sourish Banerjee,[1] Ann N. Chiaramonti,[2] Frans D. Tichelaar,[3] Kees Beenakker,[1] and Ryoichi Ishihara[1]
[1]*Faculty of Electrical Engineering, Mathematics and Computer Science, Delft Institute of Microsystems and Nanoelectronics, Delft University of Technology, Feldmannweg 17, 2628CT Delft, The Netherlands*
[2]*Applied Chemicals and Materials Division, Material Measurement Laboratory, National Institute of Standards and Technology, 325 Broadway St., Boulder, Colorado 80305, USA*
[3]*Faculty of Applied Physics, National Centre for High Resolution Electron Microscopy, Kavli Institute of Nanoscience, Delft University of Technology, Lorentzweg 1, 2628CJ Delft, The Netherlands*

(Received 30 April 2014; accepted 28 June 2014; published online 11 July 2014)

While carbon nanotubes (CNT) have been suggested as thermal management material for integrated circuits, the thermal properties, and, especially, the thermal boundary resistance (TBR) of as-grown CNT fabricated at low temperature have hardly been investigated. Here, the thermal resistance of CNT vias, with different bundle lengths and diameters fabricated at 500 °C using chemical vapour deposition, are investigated using the 3ω-method. It was found that the thermal resistance hardly changes with length except for the smallest bundle diameter of 2 μm, indicating that the TBR (10^9–10^{10} K/W per tube) dominates the thermal conduction. This is in contrast to the electrical resistance and temperature coefficient of resistance, both of which clearly increase with length. From the slope of the thermal resistance versus length of the 2 μm wide bundles, the thermal conductivity of the CNT was estimated to be 1.4–2.8 W/mK. This low thermal conductivity is attributed to the low quality of the samples as determined by Raman spectroscopy. © *2014 AIP Publishing LLC*. [http://dx.doi.org/10.1063/1.4889820]

I. INTRODUCTION

Thermal management is a serious issue in modern integrated circuits, hampering their performance and reducing reliability. In future 3D integrated circuits, which contain even more transistors per surface area, these problems will be even worse.[1] Vertically aligned carbon nanotubes (CNT) have been suggested as future thermal management material for integrated circuits, internally in the chip as vertical interconnects (vias),[2,3] and externally as heatsink[4] or thermal interface material (TIM).[5–7] To allow low-cost integration and optimum thermal contact, it is necessary to grow the CNT directly at the desired location.[8] Because the allowed thermal budget for back-end integration is limited, the CNT should be grown at relative low temperatures which generally reduces their crystallinity.[9]

While reported values for individual CNT tend to show a quite high thermal conductivity, with values greater than 3000 W/mK being reported for both single-walled and multi-walled CNT,[10,11] bundles of CNT are required in order to be able to transport enough heat.[3] For the application of vias, another reason to use bundles is to obtain a sufficiently low electrical resistivity.[3,12] Unfortunately, less thermal conductivity data are available for CNT bundles, and the data which are available show a huge spread of values, ranging from 10 W/mK to 5800 W/mK.[13–18] Moreover, none of the published results are for CNT grown at low temperatures, and directly at their desired location.

Recently, we demonstrated a vertical configuration of the well-known 3ω-method which was used to characterize the thermal conductivity of CNT bundles fabricated at 500 °C.[19] A very low thermal conductivity of 1.7 W/mK to 3.5 W/mK was obtained for the CNT, much lower than the values obtained for CNT fabricated at high temperature. We attributed this to the high defect density of the low-temperature-grown CNT.

The measured thermal conductivity consists of both the contribution of the CNT bundle, and the metal-CNT contact interface. The thermal resistance between CNT and various materials has not yet been extensively measured, but the work that has been published on single tubes indicates that the contribution of this thermal boundary resistance (TBR, thermal contact resistance or Kapitza resistance) can be substantial.[16,20,21] A high TBR has also been attributed to the poor performance of CNT-polymer composites, and techniques like functionalization, micro-wave annealing, and creation of percolating networks have been shown to improve this.[22,23] For vertically aligned CNT bundles, however, the TBR has hardly been investigated. Li *et al.*[24] investigated the TBR between CNT bundles contacted with either metal or polymers and found that the metal-CNT interface gives a higher relative TBR than the polymer-CNT interface. While Kaur *et al.*[25] demonstrated that chemical functionalization can improve the TBR of the metal-CNT interface of vertically aligned CNT.

In this work, we investigated the TBR of vertical CNT bundles fabricated at 500 °C using chemical vapour deposition (CVD), by measuring the thermal resistance versus the bundle length and extrapolating to zero length. While we

a)Electronic mail: s.vollebregt@tudelft.nl

previously found the electrical contact resistance to be small,[26] our results indicate that the TBR dominates the thermal conductance of the vertical CNT bundles.

II. EXPERIMENTAL

The CNT via test structures were fabricated as specified elsewhere.[26] In brief, 100 mm Si wafers were covered using sputtering by 500 nm Ti, 50 nm TiN, and another 100 nm Ti (which acts as a sacrificial layer). After this, 1 μm, 1.5 μm, 2 μm, or 3 μm of SiO_2 was deposited using plasma-enhanced chemical vapor deposition, and contact openings were etched using dry etching. Then, the sacrificial Ti layer was removed using 1 min 0.55% HF wet etching, and the 5 nm Fe catalyst for CNT growth was evaporated and patterned by lift-off. CNT were then grown by low-pressure CVD (LPCVD) at a temperature of 500 °C, a pressure of 8 kPa, and gas flows of 700 H_2 and 50 sccm C_2H_2. The growth time interval was set in such a way that the CNT have approximately the same length as the SiO_2 thickness. Next, 100 nm of Ti and 3 μm of Al(1% Si) were sputtered over the CNT bundles and patterned with wet etching. Finally, an etch-back to the first metal layer was performed with dry etching, in order to allow direct electrical contact to the bottom electrode.

A typical cross-section of an as-fabricated via test structure sectioned by focused ion-beam (FIB) and imaged by use of a scanning electron microscope (SEM) is shown in Fig. 1. The CNT density is estimated to be between $5 \cdot 10^{10}$ tubes/cm^2 and $1 \cdot 10^{11}$ tubes/cm^2 by counting, while the diameter is between 10 nm and 20 nm, with an average of 14 nm, as determined by transmission electron microscopy elsewhere.[26] The CNT bundle is well-aligned, with a height of 2.6 μm, which is slightly less than the oxide thickness. There is a 100 nm to 200 nm gap between the CNT bundle and the surrounding SiO_2, reducing the heat loss of the bundle to the surrounding SiO_2.

Measurements were performed using a vertical 3ω-method as described elsewhere.[19] In short, a bundle of vertically aligned CNT is suspended between two metal contacts, which are assumed to be at T_0. By driving a sinusoidal current with frequency ω through the bundle, power is pumped with double the frequency, which results in self-heating. Due to the change in resistance with temperature, a third harmonic electrical potential ($U_{3\omega}$) is generated over the bundle, which can be measured using a lock-in amplifier. In the low frequency limit, the potential depends on the sample properties as[27]

$$U_{3\omega} = \frac{4I_0^3 R|R'|L}{\pi^4 \kappa S}, \tag{1}$$

in which I_0 is the rms current, R the sample electrical resistance, R' the sample temperature coefficient of resistance (TCR), L the length of the sample, κ the thermal conductivity, and S the cross-sectional area of the sample. The low frequency limit is defined by: $\lambda \gg L$, in which λ is the thermal wavelength as specified as $\lambda = \sqrt{\alpha/2\omega}$ where α is the thermal diffusivity.[27] As shown before, these samples are measured within this limit.[19]

A four-point probe measurement technique was employed in order to accurately measure the samples by use of a probe station. To characterize the electrical resistances and TCR, a semiconductor parameter analyser was used. For the thermal measurement, a SR 830 lock-in amplifier[28] at high dynamic reserve was employed. The 1 kHz sinusoid was generated using the lock-in amplifier reference signal and converted into a known current by an improved Howland current pump.

III. RESULTS AND DISCUSSION

The average electrical resistance determined from each wafer fabricated with a different CNT length is plotted in Fig. 2 as solid lines. Although the SiO_2 layer thicknesses are 1 μm, 1.5 μm, 2 μm, and 3 μm, in SEM cross-sectional images, it was observed that the CNT length was generally a few hundred nm shorter. The electrical resistance increases linearly with CNT length, which is to be expected, as the crystallinity (quality) of these low temperature grown CNT is too low to allow ballistic transport over micrometer length.[26]

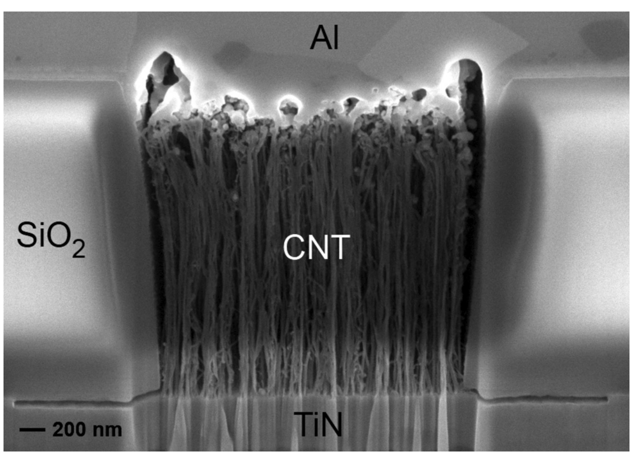

FIG. 1. SEM image of a dual-beam FIB prepared cross-section of a 2 μm wide and 3 μm deep CNT via, CNT length is estimated to be 2.6 μm.

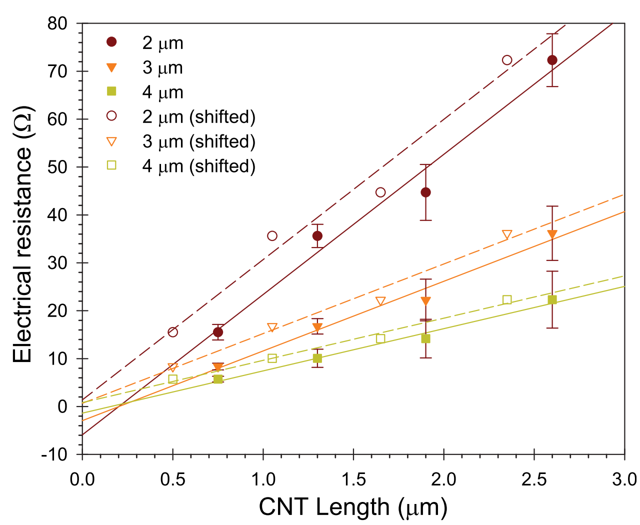

FIG. 2. Electrical CNT bundle resistance versus length for different bundle widths. Solid lines: as-measured CNT heights; dashed lines: CNT heights corrected for tip-embedding.

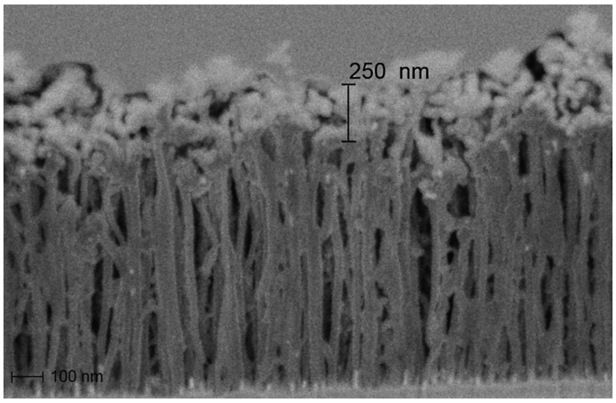

FIG. 3. Close-up of the CNT contact by cross-sectional SEM with back-scatter electron detection.

The total electrical resistance of the CNT bundle can be defined by

$$R_{bundle} = R_{C,bundle} + r_{L,bundle}L \tag{2}$$

$$= \frac{1}{N_{tubes}}(R_{C,CNT} + r_{L,CNT}L), \tag{3}$$

in which N_{tubes} is the number of CNT inside a single bundle, R_C is the electrical contact resistance between the CNT bundle and the metal contacts, and r_L the linear electrical resistivity of the CNT bundle. Upon extrapolating the electrical resistance versus length to zero for the solid lines as shown in Fig. 2, a negative electrical contact resistance is obtained which is physically impossible.

Upon close inspection of the CNT contact areas by cross-sectional SEM with back-scatter electron detection, it was found that the CNT tips are embedded in the Ti top contact metal, as shown in Fig. 3. Due to this embedding, the electrical length of the CNT is reduced by ≈250 nm. When the CNT length in Fig. 2 is reduced by the same amount (dashed lines), a small positive electrical contact resistance is obtained. We postulate that embedding of the CNT tips in the top metal contact causes this low electrical contact resistance by increasing the contact area.[26] Table I displays the fitting results of the shifted data points. As can be seen, the average contribution of R_C is one order of magnitude less than that of r_L.

By heating the wafer to 190 °C and cooling back down in steps to 25 °C while measuring the electrical resistance, the TCR of the CNT bundle resistance can be obtained.

TABLE I. Linear fitting parameters of the electrical resistance measurements and calculated per tube properties.

Bundle width (μm)	$R_{C,bundle}$ (Ω)	$r_{L,bundle}$ (Ω/μm)	$R_{C,CNT}$ (kΩ)	$r_{L,CNT}$ (kΩ/μm)
2	1.4	29	5.6	117
3	0.7	14	6.3	131
4	0.8	8.8	13	141
Average			8.3	130

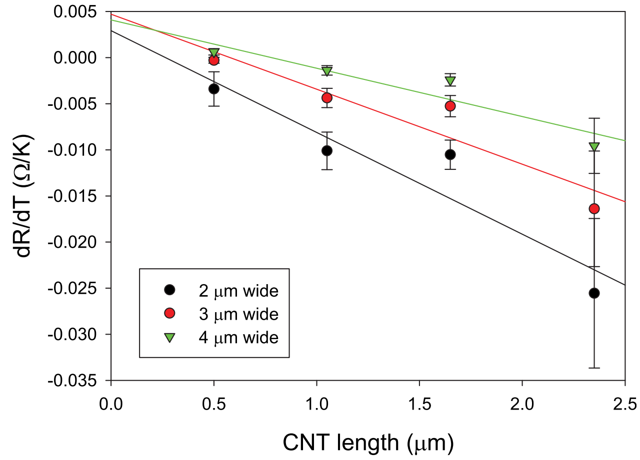

FIG. 4. CNT bundle TCR versus length for different bundle widths. The solid line is obtained by linear least-squares fitting.

As was demonstrated elsewhere, the CNT bundle electrical resistance has a linear response with temperature, and decreases with increasing temperature.[29] For CNT with many defects, this behaviour can be explained by using variable range hopping and fluctuation induced tunnelling as conduction mechanisms.[30,31] The average TCR in Ω/K for the CNT bundles used in this work for each bundle length and width are shown in Fig. 4. As can be seen, the gradient increases (becomes more negative) with increasing CNT length. As shown before, the TCR in ppm/K remains constant for CNT bundle with these lengths and widths.[29]

With the electrical resistance and its rate of change with temperature known, the 3ω-technique summarized above in Eq. (1) was implemented. An example of the behaviour of $U_{3\omega}$ as function of the applied current for 2 μm wide bundles is shown in Fig. 5 for three different CNT lengths (depicted by the oxide thickness of the samples). The equation predicts a power-law behaviour with an exponent of 3.[27] This is close to that of the data, which can be fitted by a power-law with $n = 2.8$. For all measurements, the current range was selected in such a way that the resulting data could be fitted with an

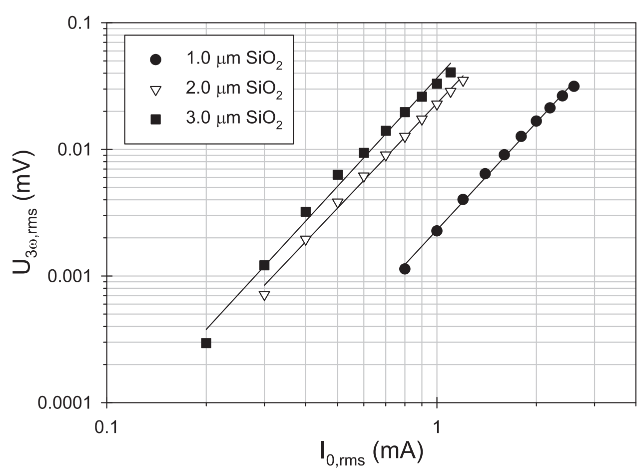

FIG. 5. Third harmonic potential versus applied current for samples with 2 μm wide vias and different CNT lengths. The solid line indicates a power-law fit with exponent $n = 2.8$.

exponent close to 3 in order to prevent errors due to self-heating of the bundles.

With the electrical resistance and TCR of each individual CNT bundle (i.e., not the average data), the thermal performance of each measured bundle with different length and width could be obtained. By removing the length and area from Eq. (1), the thermal resistance of each sample can be calculated. Here, $\Re$ is used to denote thermal resistance to avoid confusion with the electrical resistance R:

$$\Re_{bundle} = \frac{\pi^4 U_{3\omega}}{4 I_0^3 R |R'|}. \tag{4}$$

For each CNT bundle length and width, $\Re_{bundle}$ was measured for five different samples. Fig. 6 displays the average measured thermal resistances for each different bundle width, plotted against the bundle length.

Similar to the electrical resistance, the thermal resistance of a CNT bundle ($\Re_{bundle}$) can be defined by a boundary resistance ($\Re_C$) and a length-dependent term

$$\Re_{bundle} = \Re_C + \frac{L}{\kappa_{CNT} S}. \tag{5}$$

From the measurement results displayed in Fig. 6, it appears that the thermal contact resistance dominates the thermal behaviour of the 3 μm and 4 μm wide via, as the thermal resistance hardly changes with length. This is in strong contrast to the electrical resistance and thermal gradient of the electrical resistance, both of which show a significant change with length, as shown in Figs. 2 and 4. The 2 μm wide bundle, on the other hand, displays a clear length dependency of the thermal resistance. The $\Re_C$ of the measured CNT bundles appears to be in the order of 10^6 K/W, which translates into a per-tube TBR of 10^9 K/W to 10^{10} K/W, which is considerable higher than the TBR values found in literature for individual tubes and fibres, which are 10^6 K/W to 10^7 K/W.[16,20,21]

The high TBR thus appears to dominate the thermal resistance of the measured CNT vias. It has been shown that a metal-CNT contact can have a large TBR due to the difference in heat carriers, which are phonons in CNT and electrons in metals, resulting in a weak coupling.[24] Chemical functionalization to covalently bond the CNT to the metal interface has been shown to improve the TBR.[25] However, as the electrical contact resistance of these CNT is low, and Ti has been shown to have good wettability to CNT,[32] we postulate that the CNT top contact is already coupled strongly to the metal. This is confirmed by cross-sections made by cleaving the wafer, in which CNT adhere strongly to the top contact and detach from the TiN substrate. Another explanation for the high TBR is the low contact area, especially at the bottom contact. It has been shown that coating the ends of a CNT with metal can improve the heat transfer between the CNT and the metal.[16]

Using the TCR and $U_{3\omega}$ measurement data, together with Eq. (1), the thermal conductivities of the CNT inside the bundle can be obtained. The bundle length L was assumed to be equal to the electrical length used to determine the electrical contact resistance. As the CNT bundle is sparse, the actual cross-sectional area is not equal to that of the opening etched in the oxide. The following equation was used to approximate the cross-sectional diameter of the bundle ($S_{CNT,bundle}$):

$$S_{CNT,bundle} = \frac{\pi d^2}{4} D w^2, \tag{6}$$

in which d is the average CNT diameter (14 nm), D the bundle density, and w is the width of the opening.

Fig. 7 displays the average calculated thermal conductivities based on the assumptions mentioned in the previous paragraph. The values range roughly from 0.5 W/mK to 1.5 W/mK. For the 2 μm bundles, the value is constant, except for the shortest via, while the thermal conductivity increases for the 3 μm and 4 μm wide vias. This increase is caused by the more or less constant thermal resistance for these vias. The contribution of the CNT is thus shadowed by the large TBR. An estimation of the contribution of the CNT can be made from the slope of $\Re_{bundle}$ for the 2 μm via in Fig. 6, which is $1.13 \cdot 10^6$ K/μmW. Using the approximate area from Eq. (6) in combination with Eq. (5), this results in

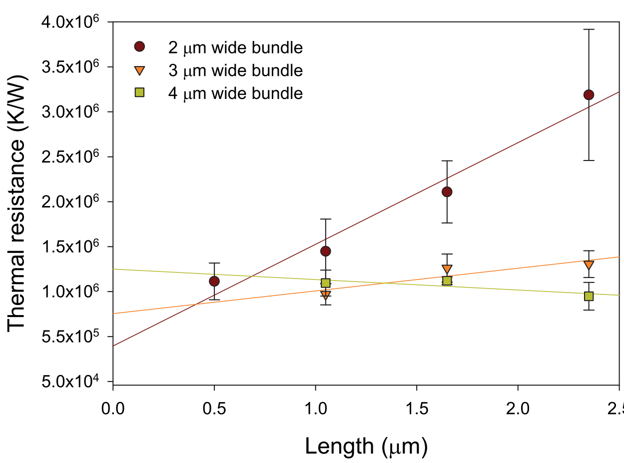

FIG. 6. Average thermal resistance for each bundle length and width, plotted against the length of the bundle.

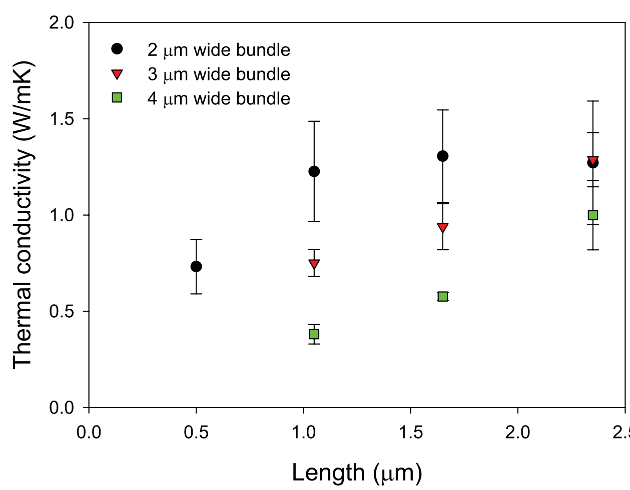

FIG. 7. Average calculated thermal conductivity for each bundle length and width and assuming a density of 10^{11} tubes/cm^2, plotted against the length of the bundle.

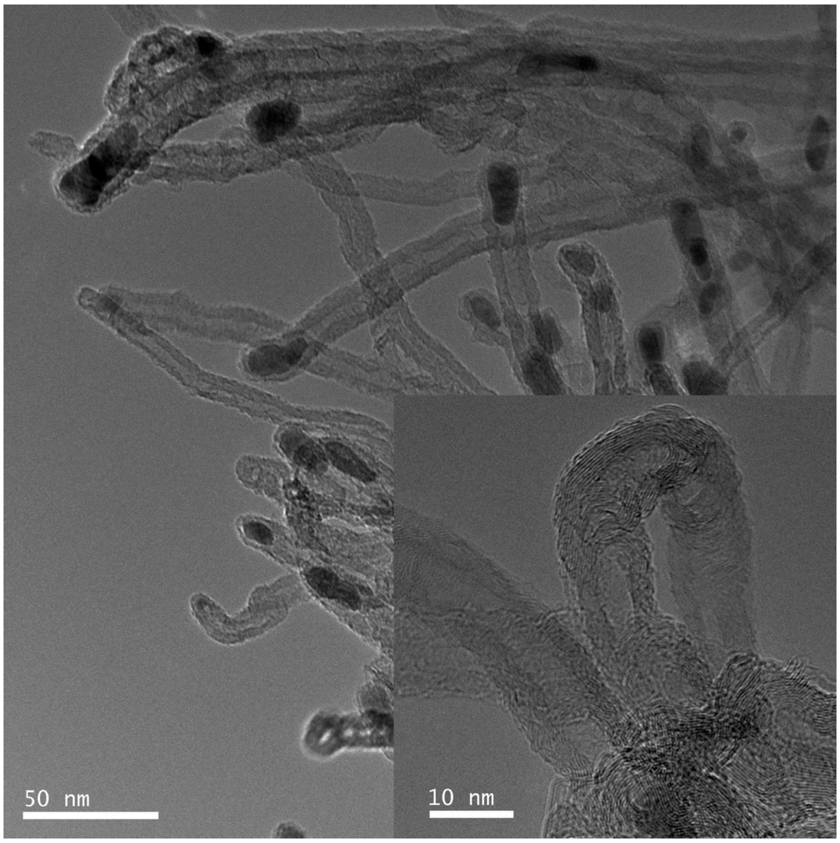

FIG. 8. TEM image of CNT grown under the exact same conditions and scraped onto a TEM grid; inset: high resolution image of part of a CNT showing the fringes of the CNT walls.

a thermal conductivity for the CNT bundle between 1.4 W/mK and 2.8 W/mK for the estimated range of densities.

The values for the thermal conductivity are lower than values previously reported, obtained from CNT fabricated at higher temperatures, which are typically between 30 W/mK and 600 W/mK.[13–15,17,18] The growth temperature used to fabricate the CNT in this study is much lower than growth temperatures previously reported. As the crystallinity (quality) of a CNT is generally inversely proportional to the deposition temperature,[9] it can be assumed that the quality of these low temperature grown CNT is lower.

Transmission electron microscope (TEM) images of CNT fabricated under the exact some conditions as used here and scraped onto a TEM grid are shown in Fig. 8. The tip-grown CNT, apparent from the catalyst particles residing at the tip, have many bamboo-crossings, and the walls show many bends. From a high resolution TEM close-up, it becomes apparent that there are many bends on the nanometre scale in the CNT walls, which suggest defects.

In order to get a more quantitative indication of the amount of defects, Raman spectroscopy was performed using a laser with 514 nm wavelength. A typical Raman spectra is shown in Fig. 9. The broad and high magnitude D-band (1350 cm^{-1}), which is associated with defects, already suggests a low sample quality.[33] As the broad band around 1600 cm^{-1} is actually a convolution of the G-band (1584 cm^{-1}, associated with the sp^2 carbon bond) and the so-called D'-band (1620 cm^{-1}, again related to defects[34]), appropriate fitting is required in order to determine the magnitude of the individual bands.[9] In order to improve the fitting two additional bands around 1200 cm^{-1} and 1500 cm^{-1} have been included, as suggested by Ferrari and Robertson.[35] From the intensity ratio of the D and G-bands, the in-plane ordering length, L_a, of a graphitic layer can be determined using an empirical formula[35,36]

$$L_a = \frac{C(\lambda)I(G)}{I(D)}, \tag{7}$$

in which $I(D)$ and $I(G)$ are the intensity ratios of, respectively, the D and G-band, and the constant $C(514\,\mathrm{nm}) \sim 4.4\,\mathrm{nm}$. The average $I(G)/I(D)$ ratio obtained from three different measurements performed on the same sample is 0.59, which, using Eq. (7), results in an L_a of approximately 2.6 nm. Due to this

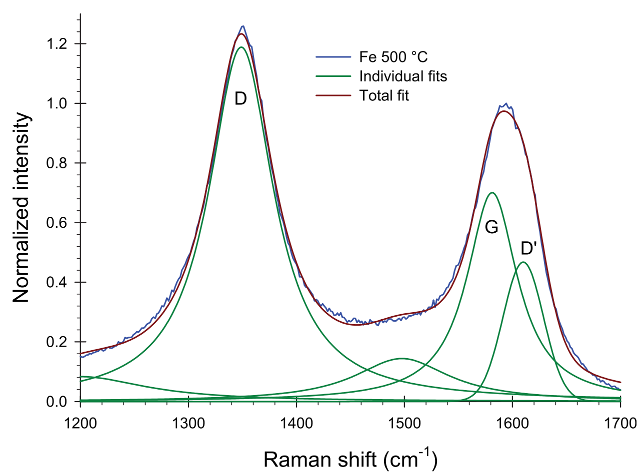

FIG. 9. Raman spectra of CNT grown at 500 °C normalized to the magnitude of the combined G and D' band, with fitting performed as described elsewhere.[9]

small ordering length, the phonon mean free path can be assumed to be short. Indeed, the reported thermal conductivities here are closer to that reported before for carbon nanofibres (10 W/mK), which were found to have a phonon mean free path of just a few nm,[16] even though these samples consist of multi-walled CNT.

In order to improve the quality of the CNT, the growth temperature could be increased, if this is compatible with the envisioned application. Otherwise, special deposition techniques using localized heating of the catalyst layer or a remote plasma have been shown to give higher quality CNT at moderate low substrate temperatures.[37,38] Tuning parameters like pressure and ratio of the growth recipe can also improve the quality of the CNT.[39,40] Effort should thus be put in developing CNT growth processes that yield a substantial higher quality, while maintaining a low enough deposition temperature. Once the material quality is improved, it can be expected that the phonon mean free path, and thus the thermal conductivity, of the individual CNT will improve significantly.

IV. CONCLUSION

The thermal resistance of CNT bundles fabricated at 500 °C was investigated using the vertical 3ω-method. While the electrical resistance and the thermal coefficient of electrical resistance displayed a clear length dependency, the thermal resistance was found to be constant with the length of the bundle, except for the smallest bundle diameter of 2 μm. This is attributed to a dominant thermal boundary resistance, estimated to be 10^9 K/W to 10^{10} K/W per tube. From the slope of the thermal resistance versus length of the 2 μm wide bundle, the thermal conductivity of the CNT was determined to be between 1.4 W/mK and 2.8 W/mK. This low value is likely caused by the short phonon mean free path, which results from the low CNT growth temperature causing many defects in the CNT shells as shown by TEM and Raman spectroscopy.

ACKNOWLEDGMENTS

Part of the work has been performed in the project JEMSiP_3D, which is funded by the Public Authorities in France, Germany, Hungary, The Netherlands, Norway, and Sweden, as well as by the ENIAC Joint Undertaking. Partial contribution of NIST, an agency of the US government; not subject to copyright in the United States.

[1]A. W. Topol, J. D. C. La Tulipe, L. Shi, D. J. Frank, K. Bernstein, S. E. Steen, A. Kumar, G. U. Singco, A. M. Young, K. W. Guarini, and M. Ieong, IBM J. Res. Dev. **50**, 491 (2006).
[2]J. Robertson, Mater. Today **10**, 36 (2007).
[3]N. Srivastava, H. Li, F. Kreupl, and K. Banerjee, IEEE Trans. Nanotechnol. **8**, 542 (2009).
[4]K. Kordás, G. Tóth, P. Moilanen, M. Kumpumäki, J. Vähäkangas, A. Uusimäki, R. Vajtaia, and P. M. Ajayan, Appl. Phys. Lett. **90**, 123105 (2007).
[5]H. Huang, C. H. Liu, Y. Wu, and S. Fan, Adv. Mater. **17**, 1652 (2005).
[6]T. Tong, Y. Zhao, L. Delzeit, A. Kashani, M. Meyyappan, and A. Majumdar, IEEE Trans. Compon. Packag. Technol. **30**, 92 (2007).
[7]K. Zhang, Y. Chai, M. M. F. Yuen, D. G. W. Xiao, and P. C. H. Chan, Nanotechnology **19**, 215706 (2008).
[8]X. J. Hu, A. A. Padilla, J. Xu, T. S. Fisher, and K. E. Goodson, J. Heat Transfer **128**, 1109 (2006).
[9]S. Vollebregt, R. Ishihara, F. D. Tichelaar, Y. Hou, and C. I. M. Beenakker, Carbon **50**, 3542 (2012).
[10]P. Kim, L. Shi, A. Majumdar, and P. L. McEuen, Phys. Rev. Lett. **87**, 215502 (2001).
[11]E. Pop, D. Mann, Q. Wang, K. Goodson, and H. Dai, Nano Lett. **6**, 96 (2006).
[12]A. Naeemi and J. D. Meindl, IEEE Trans. Electron Devices **55**, 2574 (2008).
[13]J. Hone, M. Whitney, and A. Zettl, Synth. Mater. **103**, 2498 (1999).
[14]D. J. Yang, Q. Zhang, G. Chen, S. F. Yoon, J. Ahn, S. G. Wang, Q. Zhou, Q. Wang, and J. Q. Li, Phys. Rev. B **66**, 165440 (2002).
[15]M. Horibe, M. Nihei, D. Kondo, A. Kawabata, and Y. Awano, Jpn. J. Appl. Phys., Part 1 **43**, 7337 (2004).
[16]C. Yu, S. Saha, J. Zhou, L. Shi, A. M. Cassell, B. A. Cruden, Q. Ngo, and J. Li, J. Heat Transfer **128**, 234 (2006).
[17]H. Xie, A. Cai, and X. Wang, Phys. Lett. A **369**, 120 (2007).
[18]A. E. Aliev, M. H. Lima, E. M. Silverman, and R. H. Baughman, Nanotechnology **21**, 035709 (2010).
[19]S. Vollebregt, S. Banerjee, K. Beenakker, and R. Ishihara, Appl. Phys. Lett. **102**, 191909 (2013).
[20]E. Pop, Nanotechnology **19**, 295202 (2008).
[21]J. Hirotani, T. Ikuta, and K. Takahashi, Int. J. Thermophys. **34**, 2351 (2013).
[22]W. Lin, K.-S. Moon, and C. P. Wong, Adv. Mater. **21**, 2421 (2009).
[23]M. Bozlar, D. He, J. Bai, Y. Chalopin, N. Mingo, and S. Volz, Adv. Mater. **22**, 1654 (2010).
[24]Q. Li, C. Liu, and S. Fan, Nano Lett. **9**, 3805 (2009).
[25]S. Kaur, N. Raravikar, B. A. Helms, R. Prasher, and D. F. Ogletree, Nat. Commun. **5**, 3082 (2014).
[26]S. Vollebregt, A. N. Chiaramonti, R. Ishihara, H. Schellevis, and C. I. M. Beenakker, in *12th IEEE Conference on Nanotechnology* (IEEE, 2012), pp. 424–428.
[27]L. Lu, W. Yi, and D. L. Zhang, Rev. Sci. Instrum. **72**, 2996 (2001).
[28]Commercial equipment, instruments, or materials are identified only in order to adequately specify certain procedures. In no case, does such identification imply recommendation or endorsement by the National Institute of Standards and Technology nor does it imply that the products identified are necessarily the best available for the purpose.
[29]S. Vollebregt, S. Banerjee, C. I. M. Beenakker, and R. Ishihara, IEEE Trans. Electron Devices **60**, 4085 (2013).
[30]Z. H. Khan, M. Husain, T. P. Perng, N. Salah, and S. Habib, J. Phys.: Condens. Matter **20**, 475207 (2008).
[31]R. Kamalakannan, K. Ganesan, S. Ilango, N. Thirumurugan, V. N. Singh, M. Kamruddin, B. R. Mehta, and A. K. Tyagi, Appl. Phys. Lett. **98**, 192105 (2011).
[32]S. C. Lim, J. H. Jang, D. J. Bae, G. H. Han, S. Lee, I.-S. Yeo, and Y. H. Lee, Appl. Phys. Lett. **95**, 264103 (2009).
[33]M. S. Dresselhaus, G. Dresselhaus, R. Saito, and A. Jorio, Phys. Rep. **409**, 47 (2005).
[34]S. Reich and C. Thomsen, Philos. Trans. R. Soc., A **362**, 2271 (2004).
[35]A. C. Ferrari and J. Robertson, Phys. Rev. B **61**, 14095 (2000).
[36]F. Tuinstra and J. L. Koenig, J. Chem. Phys. **53**, 1126 (1970).
[37]Y. Yamazaki, N. Sakuma, M. Katagiri, M. Suzuki, T. Sakai, S. Sato, M. Nihei, and Y. Awano, Appl. Phys. Express **1**, 034004 (2008).
[38]M. Ahmad, J. V. Anguita, V. Stolojan, J. D. Carey, and S. R. P. Silva, ACS Appl. Mater. Interfaces **5**, 3861 (2013).
[39]M. Chhowalla, K. B. K. Teo, C. Ducati, N. L. Rupesinghe, G. A. J. Amaratunga, A. C. Ferrari, D. Roy, J. Robertson, and W. I. Milne, J. Appl. Phys. **90**, 5308 (2001).
[40]T. Xu, Z. Wang, and J. Miao, in *3rd IEEE International Conference on Nano/Micro Engineered and Molecular Systems, 2008. NEMS 2008* (IEEE, 2008), pp. 471–475.